crystals

MDPI

Article

Studies on the Crystal Forms of Istradefylline: Structure, Solubility, and Dissolution Profile

Yiyun Wang [1,2], Youwei Xu [2,3], Zhonghui Zheng [2], Min Xue [1,*], Zihui Meng [1,*], Zhibin Xu [1], Jiarong Li [1] and Qing Lin [4]

[1] School of Chemistry and Chemical Engineering, Beijing Institute of Technology, Beijing 102488, China; wangyiyun@xhzy.com (Y.W.); zbxu@bit.edu.cn (Z.X.); jrli@bit.edu.cn (J.L.)
[2] Shandong Xinhua Pharmaceutical Co., Ltd., Zibo 255086, China; 3120185678@bit.edu.cn (Y.X.); zhengzhonghui@xhzy.com (Z.Z.)
[3] Xiangya School of Pharmaceutical Sciences, Central South University, Changsha 410013, China
[4] ReadCrystal Biotech Co., Ltd., Suzhou 215505, China; qing.lin@readcrystal.com
* Correspondence: minxue@bit.edu.cn (M.X.); mengzh@bit.edu.cn (Z.M.)

Abstract: Istradefylline as a selective adenosine A_{2A}-receptor antagonist is clinically used to treat Parkinson's disease and improve dyskinesia in its early stages. However, its crystal form, as an important factor in the efficacy of the drug, is rarely studied. Herein, three kinds of crystal forms of istradefylline prepared from ethanol (form I), methanol (form II), and acetonitrile (form III) are reported by use of a crystal engineering strategy. These three crystal forms were characterized and made into tablets for dissolution testing. Both the solubility and the dissolution rates were also determined. The dissolution rate of form I and form III is significantly higher than form II at pH 1.2 (87.1%, 58.2%, and 87.7% for form I, form II, and form III, respectively), pH 4.5 (88.1%, 58.9%, and 87.1% for form I, form II, and form III, respectively) and pH 6.8 (87.5%, 58.2%, and 86.0% for form I, form II, and form III, respectively) at 60 min. Considering the prepared solution and the proper dissolution profile, form I is anticipated to possess promising absorption for bioavailability.

Keywords: Parkinson's disease; istradefylline; solubility; crystal form; dissolution

Citation: Wang, Y.; Xu, Y.; Zheng, Z.; Xue, M.; Meng, Z.; Xu, Z.; Li, J.; Lin, Q. Studies on the Crystal Forms of Istradefylline: Structure, Solubility, and Dissolution Profile. *Crystals* **2022**, *12*, 917. https://doi.org/10.3390/cryst12070917

Academic Editors: Abel Moreno and Brahim Benyahia

Received: 15 April 2022
Accepted: 26 June 2022
Published: 28 June 2022

1. Introduction

The adenosine A_{2A}-receptor is closely related to Parkinson's disease (PD). A suitable antagonist could enhance the function of dopamine on D2 receptor neurons and result in some anti-Parkinson's effect [1–6]. Istradefylline (Figure 1) (KW-6002, (*E*)-8-(3,4-dimethoxystyryl)-1,3-diethyl-7-methyl-dihydro-1*H*-purine-2,6-dione) is the first approved adenosine A_{2A}-receptor antagonist that can improve the motor function of PD patients through its neuronal activity [7,8]. Moreover, it has also received extensive attention in pharmacology. Istradefylline was reported as a promising drug for movement disorders treatment [9]. In addition, Shin-ichi Uchida reported that istradefylline enhances the anti-parkinsonian activity of low doses of dopamine agonists [10–13].

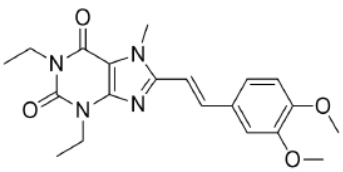

Figure 1. Chemical structure of istradefylline.

It is known that the originality of the pharmacological activity of a drug has an important influence on the effective absorption and utilization of the drug in the body.

It is remarkable that the solubility and dissolution of a drug in oral tablets significantly affects its absorption and metabolism in the body. The particle size and crystal form of a drug also affect pharmacological efficacy, due to their ability to alter the physicochemical properties of solubility, dissolution, and dosage forms. During the crystallization of a drug, different crystal structures can be formed, as the packing of molecules in space change at different temperatures, solutions, and pressures [14–17]. Generally, the appearance, melting point, dissolution, and other aspects of the same drug are significantly different in diverse crystal forms, which correspondingly affect clinical efficacy [18–22]. However, there are few reports on the solubility, crystal form, and dissolution of istradefylline.

Drug crystallization form depends on many factors, such as solvent, temperature and cooling rate, stirring speed and time, water content in solvent, and impurities in product. Based on descriptions in the literature [23–27], five crystal forms of istradefylline from ethanol/THF/isopropanol/n-propanol, methanol, acetonitrile, dichloromethane, and DMF/H_2O have been reported, while the melting points, acceleration tests, and long-term stability studies of three forms have been described; namely, the melting points of form I, form II, and form III were reported as 191.93 °C, 191.14 °C, and 191.14 °C by DSC analysis, respectively. However, the particle size, physical properties, and single crystal data of crystal forms were not reported in these patents, except for PXRD. Generally, dichloromethane and DMF were excluded in the manufacturing process due to their harmful impact on the quality of the medicine of the solution.

In this paper, we primarily discuss the dissolution rate of istradefylline in consideration of its adsorption in pharmacokinetics. In order to avoid the influence of other factors, the solubility, crystal form, particle size, and physical and chemical properties of istradefylline were also studied. The solubility and crystal form of istradefylline in seven single solvents and five mixed solvents were studied in a temperature range from 293.15 K to 333.15 K. Based on the solubility and powder diffraction data, three different crystal forms of istradefylline were obtained from ethanol (form I), methanol (form II), and acetonitrile (form III). These were consistent with the three crystal forms reported by patent NO. CN104744464A [23]. In addition, all of them were characterized by solubility, HPLC analysis, TGA and FT-IR [28,29]. In order to keep the particle size and specific surface area roughly uniform, each of the istradefylline forms was ground in a mortar for five minutes before the tablet preparation. Then, the dissolution rate of istradefylline was investigated according to the "Guidelines for determination and comparison of dissolution curves of common oral solid preparations" of Chinese pharmacopoeia. In this study, the dissolution rates of form I and form III were significantly higher than that of form II. These results have guiding significance for istradefylline tablet production.

2. Materials and Methods

2.1. Materials

Istradefylline with a purity of 99.5% was provided by Shandong Xinhua pharmaceutical Co., Ltd., Zibo, China. Acetonitrile, methanol, ethanol, ethyl acetate, n-propanol, isopropanol, and n-butanol were purchased from J.T. Baker Co., Ltd. without further purification (analytical pure), Shanghai, China. Hydrochloric acid, sodium hydroxide, potassium dihydrogen phosphate, sodium acetate trihydrate, and acetic acid were purchased from Sinopharm Group Chemical Reagent Co., Ltd. without further purification (analytical pure), Shanghai, China. Lactose (Lactose Anhydrous, NF DTHV) was provided by Kerry Inc.-Rothschild, Shanghai, China. Microcrystalline cellulose (MCC, Microcrystalline Cellulose, VIVAPUR®, PH 102) was provided by J. Rettenmaier & Sohne GmbH + Co. KG, Germany. Crospovidone (PVPP, Kollidon®, CL-F) was provided by BASF SE. Magnesium stearate (LIGAMED®, MF-2-V) was provided by Peter Greven Nederland CV. Sodium laurylsulfonate (SDS) was purchased from J&K Chemicals, Beijing, China. Purified water (18.25 MΩ·cm^{-1}) was obtained from a Millipore Mili-Q Plus water system. All saturated solutions prepared for HPLC detection were filtered through 0.22 μm filter membrane before usage.

2.2. HPLC analysis

The qualitative and quantitative determinations of istradefylline were performed on a Shimadzu HPLC system (Kyoto, Japan) comprising of two LC-20AT pumps, one SPD-20 UV detector, and a SIL-10A auto-sampler. The liquid chromatographic condition was optimized on an Agilent ZORBOX C18 chromatographic column (150 mm × 4.6 mm, 5 μm) with acetonitrile and water (60/40, *v*/*v*) as the stationary and mobile phase, respectively. The flow rate was confirmed as 1.0 mL·min^{-1}, while the UV-determined wavelength was 355 nm, and the sample injection volume was 20 μL.

2.3. Solubility of Istradefylline in Diverse Organic Solvents and Solvent Mixtures with Water

A certain amount of istradefylline powder was placed into a glass vial with 10 mL of acetonitrile, methanol, ethanol, ethyl acetate, n-propanol, isopropanol, n-butanol, methanol/water (30/70, *v*/*v*), ethanol/water (24/76, *v*/*v*), ethanol/water (55/45, *v*/*v*), acetonitrile/water (25/75, *v*/*v*), and acetonitrile/water (58/42, *v*/*v*), respectively. Then, the vials were incubated in a thermostat water bath for 12 h with magnetic stirring at 293.15 K, 303.15 K, 313.15 K, 323.15 K, and 333.15 K, each measured by a thermometer inside each glass vial. The temperature fluctuation of the thermostat water bath was controlled within ±0.5 K with temperature uncertainty of ±0.1 K. Then, all solutions were left to stand for a further 12 h at the corresponding temperature until the dissolution equilibrium was obtained. Then, 2 mL of supernatant from each vial was withdrawn by a syringe with a 0.22 μm filter membrane for HPLC analysis. All of the experiments were carried out three times simultaneously to obtain data averages (Table S1).

2.4. Preparation of Single Crystal

First, 1 g istradefylline was added into each of three 100 mL single-mouth flasks with 20 mL ethanol, 50 mL methanol, or 20 mL acetonitrile, respectively. Then, the mixture was stirred and heated at 78 °C, 64.5 °C and 81.0 °C, respectively, until completely dissolved, followed by being cooled down to room temperature. Stirring continued for 2 h for crystallization. Consequently, forms I, II, and III of istradefylline were obtained by filtration.

2.5. X-ray Diffraction

Single-crystal X-ray diffraction data were collected using a Bruker apex2 X-ray diffractometer equipped with a Mercury CCD detector with graphite monochromated Mo-K α radiation (λ = 0.71073 Å) at 296 K. The structures were solved by direct methods and refined by full-matrix least-squares on F2 values (SHELXL-97). Non-hydrogen atoms were refined anisotropically. Hydrogen atoms were fixed at calculated positions and refined using a riding mode. Powder X-ray diffraction (PXRD) patterns of samples were collected on a Bruker D8 Focus X-ray diffractometer with Cu Kα radiation (λ = 1.54 Å) at a scanning rate of 0.02° s^{-1} from 5° to 50° in 2θ.

2.6. Differential Scanning Calorimetry (DSC) and Thermogravimetric Analysis (TGA)

The DSC and TGA was determined by TGA/DSC1/1100LF(Mettler Toledo, Switzerland). The temperature range was 25~1100 °C; temperature accuracy was ±0.3 °C; calorimetric accuracy was ±1%; balance sensitivity was 0.1 μg; heating rate was 0.1~100 K/min.

The experiment was performed under N_2 atmosphere at 1 atm with a heating rate of 10 °C/min in a temperature range of 30~400 °C.

2.7. Fourier-Transform Infrared Spectral Analysis (FT-IR)

FT-IR analysis was collected in a range of 3600–1600 cm^{-1} using KBr pellets and a Thermo iD7 ATR infrared spectrometer (Thermo Fisher Technology (China) Co., Ltd., Shanghai, China).

2.8. Particle Size and Specific Surface Area Analysis (BET)

The particle sizes of forms I/II/III were determined by a Malvern 2000 laser particle size analyzer (Malvern, England). The specific surface areas (N_2 adsorption) of forms I/II/III were detected by the specific surface-area analyzer BK200B (Beijing Jingwei Gaobo Science and Technology Co., Ltd., Beijing, China.).

The samples were mixed thoroughly and evenly (loose clumps were gently pressed with a spoon to completely disperse) and flatly laid on the sample table of the Scirocco 2000 dry sampler. Vibration injection speed was 30~80%; relaxation-dispersed air pressure was 2.5 bar; cost of shading was 1~5%; measuring time was 10 s; background time was 10 s.

Specific surface-area analysis was performed under N_2 adsorption with adsorption temperature of 77.35 K on a BK200B using the static capacity method, while the temperature was controlled at 40 °C for 360 min.

2.9. Dissolution Study

The instruments used for tablets included a circulating water vacuum pump (SHB-III, Zhengzhou Great Wall Science, Industry and Trade Co., Ltd., Zhengzhou, China), an electrothermal blast drying box (GZX-9240MBE, Shanghai Boxun Industrial Co., Ltd., Shanghai, China), an electronic balance (PB3002-S, METTLER TOLEDO), a constant-temperature magnetic stirrer (DF-101S, Zhengzhou Great Wall Industry and Trade Co., Ltd.), an ultraviolet-absorption spectrophotometer (UV1800, Shimadzu, Kyoto, Japan), a dissolution tester (SNTR-8400AT, Shimadzu), a single-stamping-sheet machine (YP-1, HangZhou XuZhong Food Machinery Co., Ltd.), and a high-efficiency coating machine (JCB/K-3/5/10, Wenzhou Jianpai Pharmaceutical Machinery Co., Ltd., Wenzhou, China, nozzle diameter of 1 mm).

In order to prepare the istradefylline tablets, a prescribed amount of istradefylline was weighed and ground in a mortar for 5 min. Lactose, microcrystalline cellulose PH102, and PVPP were weighed and mixed with istradefylline by hand for 3 min. Then, magnesium stearate (MS) was weighed and added into the above mixture and mixed again by hand for 3 min. A single-stamping-sheet machine (mold circular concave Φ7.1 mm, tablet weight 140 mg, tablet hardness −5 kp) was used for tableting. The coating liquid prepared by Opadry 03K19229 (solid content: 8%) was coated on a high-efficiency coating machine. The inlet air temperature was 70 °C, the atomization gas pressure was 0.3 MPa, the rotation speed was 8 rpm, and the spraying speed was 7 rpm. Coating-weight gain was controlled at about 3%. The batch size was 1000 pieces. The tablet speed was 1000 tablets/h, and the coating batch was 800 tablets/batch. The spray speed was 7.0 g/min. The prescription ingredients are shown in Table 1 in detail.

Table 1. Prescription ingredients list.

Process	Material Name	Function	Batch Size/g	Proportion/%
Tablet	Istradefylline	Drug	20.00	14.29
	MCC PH102	Fillers	67.50	48.21
	Lactose	Diluents	42.00	30.00
	PVPP	Disintegrant	9.80	7.00
	MS	Lubricants	0.70	0.50
	Total		140.0	100.0
Coating	Opadry	Materials	5.2	3%
Single piece of content	Purified water	Solvent	59.8	Final removal
Actual use (1.2 times preparation)	Opadry	Materials	54.4	3%
	Purified water	Solvent	626.0	Final removal

According to the dissolution and release determination method (Chinese Pharmacopoeia 2020 Edition, general rule of the fourth part 0931, second method), six tablets of istradefylline were put into a beaker filled with 900 mL buffer solution of pH 1.2, pH 4.5, and pH 6.8, while the rotation speed was fixed at 75 r/min. Then, 10 mL samples were

taken out at 5 min, 10 min, 15 min, 30 min, 45 min, and 60 min and filtrated with 0.22 μm filter membrane. Then, 2 mL filtrate was diluted to 10 mL with a diluent (acetonitrile-water (50:50)), and the test sample was obtained. Next, 25 mg istradefylline was precisely weighed and dissolved into 25 mL acetonitrile in a volumetric flask. Then, 1 mL istradefylline solution was diluted to 5 mL with a diluent (acetonitrile-water (50:50)), and the solution was mixed. Next, 2 mL solution was precisely measured and transferred into a 10 mL volumetric flask. Then, 2 mL dissolution medium was added, and the solution was diluted to scale with a diluent (acetonitrile-water (50:50)), upon which the reference solution was obtained.

The same amount of diluent (acetonitrile-water (50:50)) was added to the two cuvettes, and then they were placed in channel 1 and channel 2 of UV-Vis spectrophotometer, respectively. After the instrument was zeroed, the reference solution and sample solution were placed in channel 2 and measured at a wavelength of 362 nm. Each group of samples was repeatedly tested six times, and the RSD of all samples at each time point was less than 10%, which proved that each sample had good uniformity.

Computational Formula:

$$\text{Dissolution} = \frac{A_{test} \times C_{reference} \times 5 \times 900}{A_{reference} \times 20} \times 100\%$$

$$\text{Cumulative dissolution} = A_n + \frac{(A_n - 1 + \ldots\ldots + A_1) \times 10}{900}$$

where A_{test} is UV absorbance of sample, $A_{reference}$ is UV absorbance of reference substance, $C_{reference}$ is concentration of reference substance.

3. Results and Discussion

3.1. Solubility of Istradefylline

A perfect chromatogram of istradefylline as a symmetrical sharp peak was obtained, as shown in Figure 2. The relationship between the chromatogram peak area and concentration expressed as calibration curve is graphically displayed in Figure 2. The linear fitting equation was Y = 4.42X + 7.06 with a concentration range of 0.001 mg·mL^{-1} to 0.1 mg·mL^{-1}, while the linear dependence was 0.9999. The linearity was used to calculate the istradefylline concentration in the supernatant of each vial in the experiment by HPLC detection.

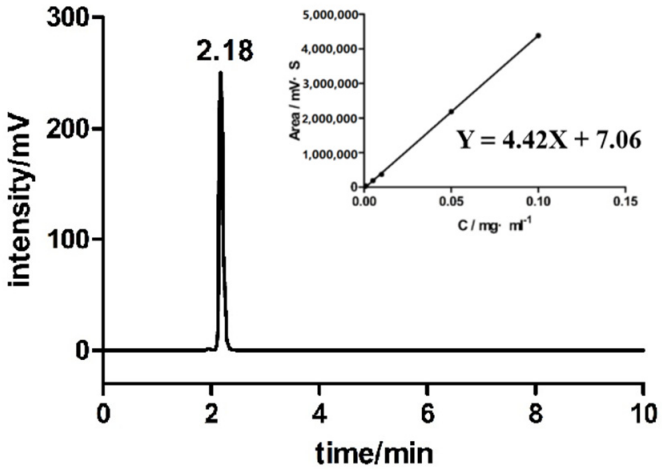

Figure 2. HPLC chromatogram of istradefylline. Insets show the linear relationship between the chromatogram peak area (Y) and the concentration (X) of istradefylline in acetonitrile.

In this study, the solubility data of istradefylline in common organic solvents in the range of 293.15 K to 333.15 K were determined by an established HPLC method with

milligram-grade usage. The solubility of istradefylline was expressed by mole fraction of the solute in the solution. The mass of the solute in the sample solution can be calculated according to Equation (1), while the concentration of istradefylline in saturated solution was estimated by the liquid chromatographic method according to the calibration curve,

$$m = c \cdot v \tag{1}$$

where m is the mass of istradefylline in saturated solution, c is the corresponding concentration, and v is the volume after diluted. The mole fraction of the solute can be readily calculated as follows:

$$x = \frac{m_1 / M_1}{m_1 / M_1 + (m_0 - m_1) M_2} \tag{2}$$

where x is the mole fraction of the solute istradefylline, m_1 is the mass of the solute calculated by Equation (1), M_1 is the molecular weight of solute, m_0 is the mass of the solution, and M_2 is the molecular weight of solvent. The precise solubility of this compound in seven single-solvents and five mixed-solvents in the range of 293.15 K to 333.15 K is recorded in Table S1. Furthermore, the temperature influence on the solubility of istradefylline was also studied. Solubility increased at an exponential rate with rising temperature in all solvents, as shown in Figure 3. Generally, the solubility of chemicals is an endothermic process, so increasing the temperature is beneficial for increasing the solubility of drugs. Besides the solubility data, which were useful in the quality control and process improvement that followed, three kinds of crystalline forms were also determined and classified in these solvents by powder X-ray diffraction method.

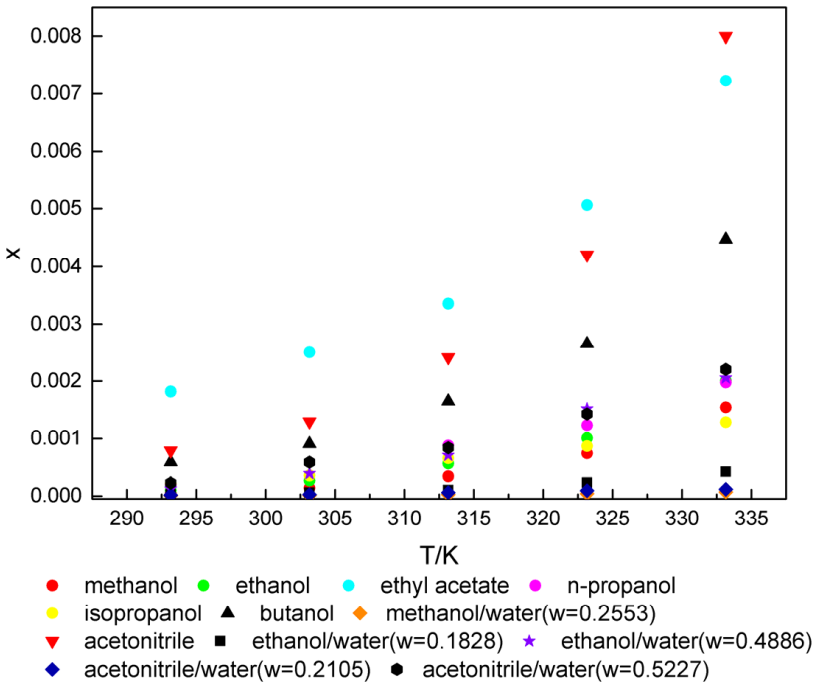

Figure 3. Temperature dependence of mole fraction of istradefylline in several solvents.

It is known that the solubility of istradefylline is very low in aqueous media in the pH range from 1.0 to 12.0, so the solubility of istradefylline in aqueous solutions of different pH was tested. The test results were shown in Table 2. From the test results, it can be seen that the solubility of istradefylline decreased when the pH increased, since istradefylline is a weakly alkaline drug that has greater solubility in acidic solutions.

Table 2. Solubility of istradefylline in different pH at 293.15 K.

pH	Solubility of Istradefylline (μg/mL)
1	0.41
2	0.39
3	0.32
4	0.31
7	0.27
8	0.18
10	0.11
12	0.10

3.2. Powder X-ray Diffraction

The istradefylline crystalline solids from the saturated solutions were characterized by X-ray powder diffraction (Figure 4). Three forms can be clearly distinguished from the significant differences present among their diffraction patterns. Form I could be obtained in a wide variety of solvent systems, including ethyl acetate, n-propanol, isopropanol, n-butanol, ethanol, ethanol/water (w = 0.1828), and ethanol/water (w = 0.4886). Its powder diffraction pattern is characterized by peaks at 2θ = 6.98°, 11.02°, 13.98°, 15.68°. Form II crystallized in methanol and methanol/water (w = 0.2553). Its characteristic diffraction peaks can be found at 2θ = 8.68°, 11.86° and 12.12°. Form III, obtained in acetonitrile, acetonitrile/water (w = 0.2105), and acetonitrile/water (w = 0.5127), shows characteristic diffraction peaks at 2θ = 9.74°, 10.24°, 12.38° and 25.07°. These results were consistent with the three forms disclosed by patent number CN104744464A.

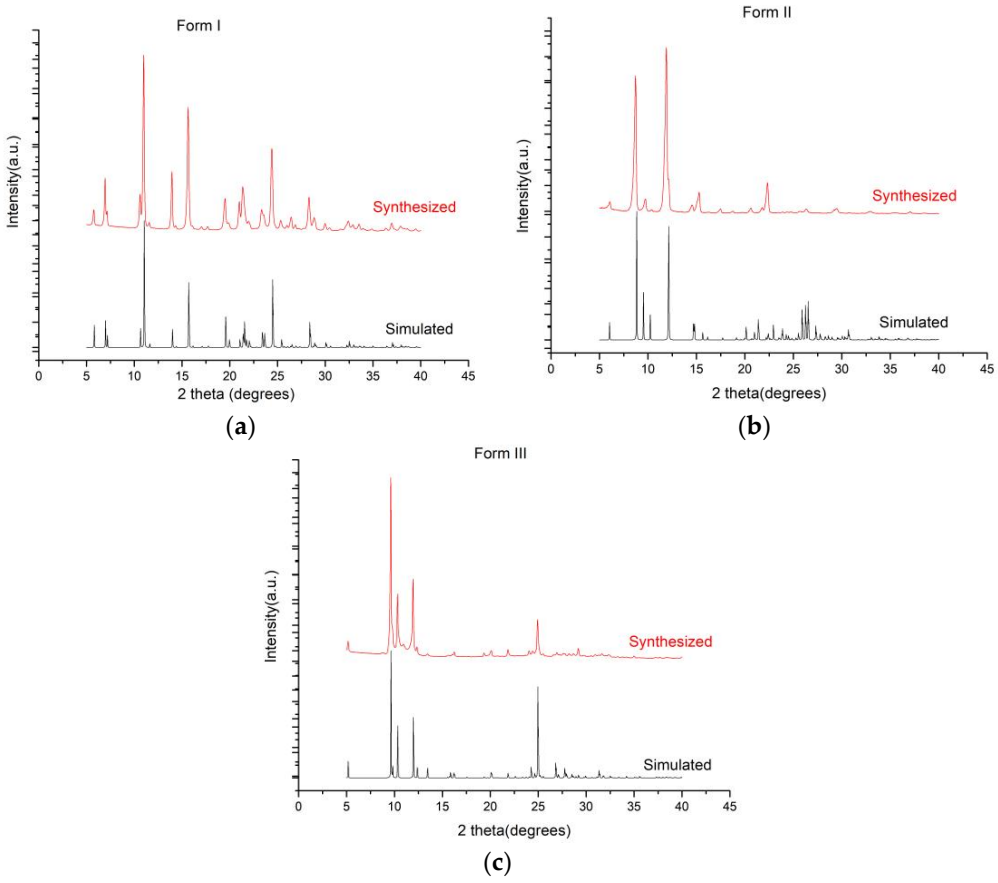

Figure 4. Comparison of powder X-ray diffraction (after grinding) and crystallographic data of istradefylline. (**a**) Form I made in ethanol; (**b**) Form II made in methanol; (**c**) Form III made in acetonitrile.

3.3. Single-Crystal X-ray Diffraction

For further study, three forms were obtained using ethanol, methanol, and acetonitrile as the crystallization solvents, respectively (CCDC number: 2043873-2043875). Their crystal structure and crystallography data are shown in Figures S1–S3 and Table 3.

Table 3. Crystallographic data and structure refinement parameters.

Compounds	Form I	Form II	Form III
Chemical formula	$C_{20}H_{24}N_4O_4$	$C_{20}H_{26}N_4O_5$	$C_{22}H_{29}N_5O_5$
Formula weight	384.43	402.45	443.50
Crystal system	monoclinic	monoclinic	monoclinic
Space group	*P*21	*P*21/*c*	*P*21/*m*
a/Å	13.6762(17)	4.5436(5)	9.430(9)
b/Å	4.7483(7)	23.776(2)	7.129(7)
c/Å	16.464(2)	18.6282(17)	17.587(18)
α/°	90	90	90
β/°	112.39(4)	95.065(7)	103.514(10)
γ/°	90	90	90
vol/Å3	988.5(2)	2004.6(3)	1149.5(19)
Z	2	4	2
ρcalcg/cm^3	1.292	1.334	1.281
Gof	1.017	1.036	1.052
R	R1= 0.0552, wR2 = 0.1107	R1 = 0.0888, wR2 = 0.2892	R1 = 0.083, wR2 = 0.27

According to the crystallographic data and structure refinement parameters, three forms can be effectively distinguished. From the single-crystal structure, it can be seen that form I was pure crystal, form II was monohydrate crystal, and form III was monohydrate of acetonitrile solvent complex. The three forms were all monoclinic systems with different space groups, with form I, II and III exhibiting *P*21, *P*21/*c* and *P*21/*m*, respectively. The molecular packing and intermolecular interactions of the three forms were different (Figure 5). Form I has strong intermolecular hydrogen bonds between oxygen atoms and the nearby hydrogen on the other side of the molecule (C=O . . . H, 2.37 Å and 3.16 in form I), without π-π stacking. Form II and form III have hydrogen bonds between oxygen atoms and the nearby hydrogens of water molecules (O5=O2 . . . H, 2.878 Å in form II and O5A=O3 . . . H, 2.955 Å in form III). Although abundant hydrogen bonds were constructed through the interactions between water molecules and the crystal of form II and form III, their bond energies of about 15~30 kJ·mol^{-1} were much lower than those of general chemical bonds. This suggests that these hydrogen bonds are fragile, and the water molecules are transferred during the drying process of istradefylline. Otherwise, form II was a head-to-head π-π interaction, and form III was a head-to-tail π-π interaction. The π-π stacking interaction of form II, at 3.55 Å, was stronger than that of form III, at 3.54 Å, between two molecules. It is well-known that π-π stacking is detrimental to the solubility of compounds. Different π-π stacking forms also have an effect on solubility, which may lead to the weak solubility and dissolution of the crystalline form II of istradefylline.

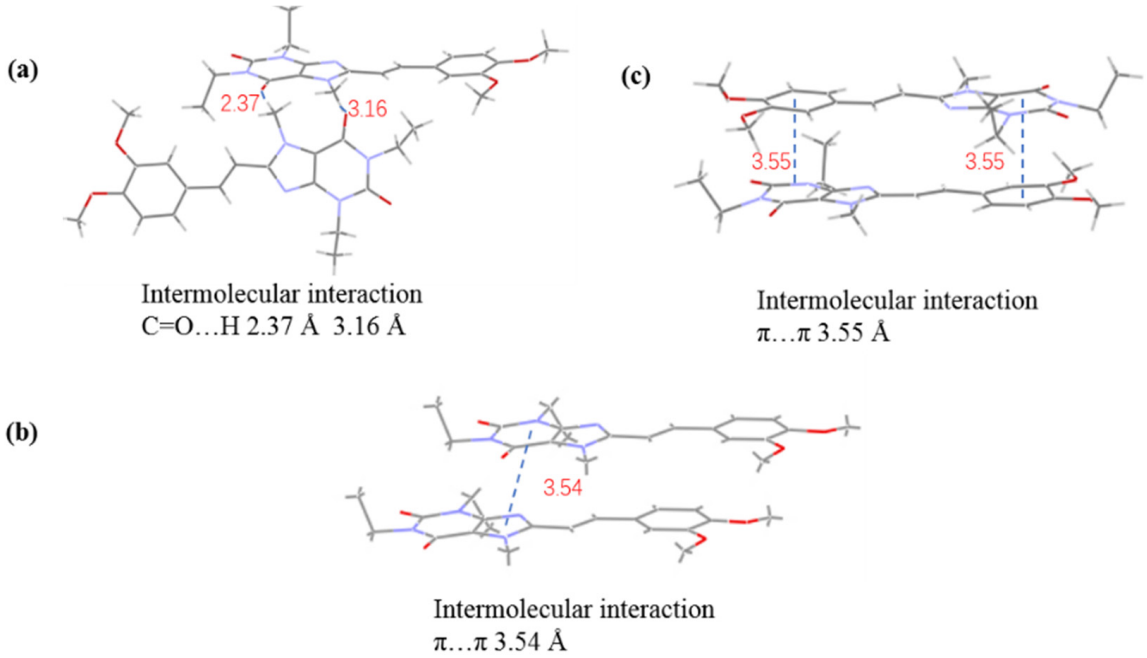

Figure 5. Single-crystal molecular structure of istradefylline in (**a**) ethanol (form I), (**b**) methanol (form II) and (**c**) acetonitrile (form III), respectively, and π-π stacking and hydrogen-bond lengths.

3.4. TGA

Figure S5 shows the TGA curves for form I, form II, and form III at a heating rate of 10 °C/min under N_2 atmosphere. As shown in Figure S5a, the weight loss of form I was 99.98% from 191.66 to 198.08 °C, corresponding to the degradation of istradefylline molecules. In Figure S5b, the weight loss of form II was in two stages: the first weight loss of 3.23% from 27.56 °C to 52.45 °C corresponds to the release of one H_2O molecule (calc. 4.48%), while the second weight loss occurred at or above 377.72 °C, corresponding to the degradation of istradefylline. In Figure S5c, the thermal decomposition process of cocrystal III was in two stages: the first weight loss of 15.62% from 91.16 °C to 121.02 °C corresponds to the release of one H_2O molecule and one CH_3CN molecule (calc. 13.32%), while the second weight loss occurred at or above 258.93 °C, corresponding to the degradation of istradefylline.

3.5. FT-IR Analysis

In Figure S6a, the absorbance peaks at 2966 cm^{-1}, 2935 cm^{-1}, and 2832 cm^{-1} are ascribed to the presence of the methyl or methylene group. In Figure S6b, the absorbance peaks at 3482 cm^{-1}, 2977 cm^{-1}, 2935 cm^{-1}, and 2841 cm^{-1} are ascribed to the presence of the hydroxy, methyl, or methylene group. In Figure S6c, the absorbance peaks at 2979 cm^{-1}, 2932 cm^{-1}, 2839 cm^{-1}, and 2217 cm^{-1} are ascribed to the presence of the methyl or methylene group, the absorbance peaks at 3465 cm^{-1}, 3380 cm^{-1} and 3028 cm^{-1} indicate the presence of water molecules, and the absorbance peak at 2217 cm^{-1} indicates the presence of acetonitrile molecules.

3.6. Particle Size and BET Analysis

The particle size of form I, II and III was determined with a Malvern 2000 laser particle-size analyzer, and the median particle sizes were 5.6 μm, 5.2 μm, and 7.1 μm, respectively. The specific surface areas of the three forms were 5.08 m^2/g, 5.51 m^2/g and 5.18 m^2/g, respectively. The specific surface areas of single points were 0.20000 at P/Po is 4.67 m^2/g, 4.74 m^2/g, and 4.72 m^2/g, respectively. As can be seen from the above data, the surface area was basically the same.

3.7. Dissolution Curve Test

The dissolution of istradefylline in three crystal forms was studied in a buffer solution in which pH value was fixed at 1.2, 4.5, and 6.8, corresponding to pH of digestive solutions such as gastric juice and intestinal juice. All experiments were repeated six times, as shown in Figure 6. The dissolution rates of the three crystal forms at pH 1.2 at 5 min were 72.2%, 28.3%, and 74.7%, respectively. At 60 min, the dissolution rates of form I, II, and III reached 87.1%, 58.2%, and 87.7% respectively. The dissolution rates of the three crystal forms at pH 4.5 at 5 min were 68.3%, 29.4%, and 73.2%, respectively. At 60 min, the dissolution of form I reached 88.1%, the dissolution of form II reached 58.9%, and the dissolution of form III reached 87.1%. The dissolution rates of the three crystal forms at pH 6.8 at 5 min were 69.2%, 30.3%, and 70.7%, respectively. At 60 min, the dissolution of form I reached 87.5%, the dissolution of form II reached 58.2%, and the dissolution of form III reached 86.0%. From the dissolution profile of the three crystal forms of istradefylline, it can be inferred that the dissolution of istradefylline form I, refined in ethanol, and form III, refined in acetonitrile, show good dissolution performance, while that of form II, refined in methanol, was significantly lower. Through single-crystal studies, it was found that form II has π-π stacking, and the π-π stacking interaction of form II is stronger than that of form III between two molecules. The π-π stacking leads to weak solubility and dissolution in istradefylline. These results indicate that the solvent has a direct effect on the dissolution.

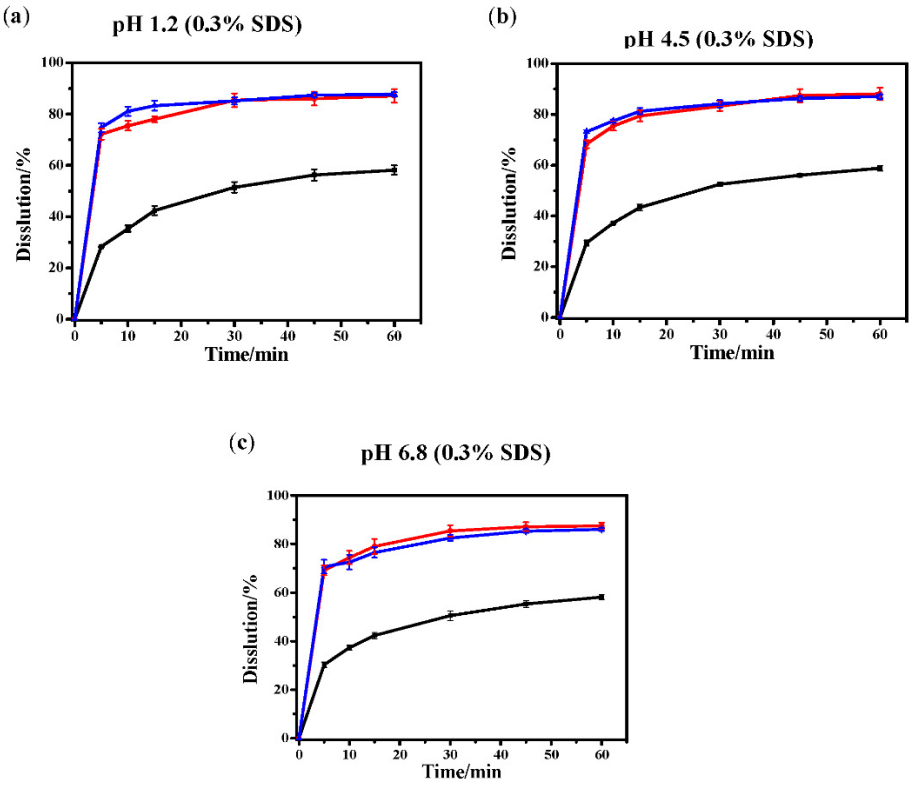

Figure 6. Dissolution curve of three crystal forms of istradefylline.

4. Conclusions

In this paper, the solubility of istradefylline in 12 kinds of solvents such as ethanol, methanol, and acetonitrile was studied, and three kinds of crystal forms were sequentially obtained in these solvents and proved by X-ray powder diffraction. Their single-crystal diffraction structure and data were also confirmed by single-crystal diffraction. Furthermore, the dissolution test was performed with tablets prepared from the three crystal forms of istradefylline, and it was found that the dissolution rates of the three crystal forms were different. Compared with form II, the dissolution rates of form I and form III were superior. Additionally, the solubility and X-ray powder diffraction data, as well as the dissolution

rates, indicated that the packing of molecules and crystal forms have notable influence on solubility and dissolution. This study offers additional insight into optimizing the crystallization process of istradefylline and improving absorption in pharmacokinetics.

5. Patents

Preparation method and application of istradefylline crystal, CN113024558A, 2021-06-25.

Supplementary Materials: The following supporting information can be downloaded at: https://www.mdpi.com/article/10.3390/cryst12070917/s1. Table S1. Solubility of Istradefylline in Twelve Different Solvents from 293.15 K to 333.15 K. Table S2. Bond Lengths for Istradefylline. Table S3. Stability data of Istradefylline (Form I of istradefylline). Figures S1–S3. ORTEP view with labeling scheme for Istradefylline. Figure S4. The surface area of three crystal forms. Figure S5. (a) The TGA curves of From I, (b) The TGA curves of From II and (c) The TGA curves of From III. Figure S6. The IR of From I, The IR of From II and The IR of From III.

Author Contributions: Conceptualization, Y.W. and M.X.; methodology, Y.W.; software, M.X.; validation, M.X.; formal analysis, Z.Z., Z.M., Z.X., J.L. and Q.L.; investigation, Y.W.; resources, Y.W.; data curation, Y.X.; writing—original draft preparation, Y.W. and M.X.; writing—review and editing, Y.W. and M.X. All authors have read and agreed to the published version of the manuscript.

Funding: This research received no external funding.

Institutional Review Board Statement: Not applicable.

Informed Consent Statement: Not applicable.

Data Availability Statement: Not applicable.

Acknowledgments: The authors wish to thank the Suzhou Jingyun Pharmaceutical Technology Co., Ltd., Suzhou ReadCrystal Biotechnology Co., Ltd. and the instrumental analysis center of Beijing Institute of Technology for their powder X-ray diffraction analysis, single crystal diffraction and so on.

Conflicts of Interest: The authors declare that they have no known competing financial interest or personal relationships that could have appeared to influence the work reported in this paper.

References

1. Zheng, J.Y.; Zhang, X.H.; Zhen, X.C. Development of Adenosine A_{2A} Receptor Antagonists for the Treatment of Parkinson's Disease: A Recent Update and Challenge. *ACS Chem. Neurosci.* **2019**, *10*, 783–791. [CrossRef]
2. Shook, B.C.; Jackson, P.F. Adenosine A_{2A} Receptor Antagonists and Parkinson's Disease. *ACS Chem. Neurosci.* **2011**, *2*, 555–567. [CrossRef]
3. Hauser, R.A.; Shulman, L.M.; Trugman, J.M.; Roberts, J.W.; Sussman, N.M. Study of istradefylline in patients with Parkinson's disease on levodopa with motor fluctuations. *Mov. Disord.* **2010**, *23*, 2177–2185. [CrossRef]
4. Tian, S.; Wang, X.; Li, L.L.; Zhang, X.H.; Li, Y.Y.; Zhu, F.; Hou, T.J.; Zhen, X.C. Discovery of Novel and Selective Adenosine A2A Receptor Antagonists for Treating Parkinson's Disease through Comparative Structure-Based Virtual Screening. *J. Chem. Inf. Model.* **2017**, *57*, 1474–1487. [CrossRef]
5. Lu, J.; Cui, J.; Li, X.H.; Wang, X.; Zhou, Y.; Yang, W.J.; Chen, M.; Zhao, J.; Pei, G. An Anti-Parkinson's Disease Drug via Targeting Adenosine A_{2A} Receptor Enhances Amyloid-β Generation and γ-Secretase Activity. *PLoS ONE* **2016**, *11*, e0166415. [CrossRef]
6. Uchida, S.I.; Soshiroda, K.; Okita, E.; Uchida, M.K.; Mori, A.; Jenner, P.; Kanda, T. The adenosine A_2A receptor antagonist, istradefylline enhances the anti-parkinsonian activity of low doses of dopamine agonists in MPTP-treated common marmosets. *Eur. J. Pharmacol.* **2015**, *747*, 160–165. [CrossRef]
7. Ko, W.K.D.; Sandrine, M.C.; Li, Q.; Yang, J.Z.; Steve, M.; Elsa, Y.P.; Erwan, B. An evaluation of istradefylline treatment on Parkinsonian motor and cognitive deficits in 1-methyl-4-phenyl-1,2,3,6-tetrahydropyridine (MPTP)-treated macaque models. *Neuropharmacology.* **2016**, *110*, 48–58. [CrossRef]
8. Matsuura, K.; Kajikawa, H.; Tabei, K.I.; Satoh, M.; Kida, H.; Nakamura, N.; Tomimoto, H. The effectiveness of istradefylline for the treatment of gait deficits and sleepiness in patients with Parkinson's Disease. *Neurosci. Lett.* **2018**, *662*, 158–161. [CrossRef]
9. Kataoka, H.; Sugie, K. Does istradefylline really have a dystonic mechanism? *J. Neurol. Sci.* **2018**, *388*, 233–234. [CrossRef]
10. Fumio, S.; Junichi, S.; Nobuaki, K.; Joji, N.; Shizuo, S.; Shunji, I.; Hiromi, N. Therapeutic Agents for Parkinson's Disease. EP0590919, 29 December 1999.
11. Li, J.; Han, Y.F.; Li, Y.X.; Chen, S.W.; Gong, P. Improved synthesis process of adenosine A_2A receptor inhibitor istradefylline. *Chin. J. Med. Chem.* **2018**, *2*, 220–224.

12. Uchida, S.I.; Soshiroda, K.; Okita, E.; Uchida, M.K.; Mori, A.; Jenner, P.; Kanda, T. The adenosine A_2A receptor antagonist, istradefylline enhances anti-parkinsonian activity induced by combined treatment with low doses of L-DOPA and dopamine agonists in MPTP-treated common marmosets. *Eur. J. Pharmacol.* **2015**, *766*, 25–30. [CrossRef] [PubMed]
13. Uchida, S.I.; Tashiro, T.; Kawai-Uchida, M.; Mori, A.; Jenner, P.; Kanda, T. The adenosine A_{2A}-receptor antagonist istradefylline enhances the motor response of L-DOPA without worsening dyskinesia in MPTP-treated common marmosets. *J. Pharmacol. Sci.* **2014**, *124*, 480–485. [CrossRef] [PubMed]
14. Huang, T.H.; Lu, D.Q.; Ling, X.Q.; Wang, X.X.; Liu, T.Q.; Shen, F.F.; He, K.F. Thermodynamic models for determination of the solid-liquid equilibrium of Istradefylline in ethyl acetate plus (isopropanol, tetrahydrofuran, acetone) binary solvent mixtures. *J. Chem. Thermodyn.* **2017**, *111*, 31–40. [CrossRef]
15. Ge, Y.H.; Li, T.T.; Cheng, J.J. Crystal Type I of Azilsartan Polymorphs: Preparation and Analysis. *J. Cryst. Process. Technol.* **2016**, *6*, 1–10. [CrossRef]
16. Yadav, M.R.; Shaikh, A.R.; Ganesan, V.; Giridhar, R.; Chadha, R. Studies on the crystal forms of pefloxacin: Preparation, characterization and dissolution profile. *J. Pharm. Sci.* **2008**, *97*, 2637–2648. [CrossRef]
17. Ganesan, V. Studies on the crystal forms of moxifloxacin: Preparation, characterization and dissolution profile. *Pharm. Anal. Acta* **2013**, *4*, 135.
18. Zhang, X.M.; Sun, F.X.; Zhang, T.T.; Jia, J.T.; Su, H.M.; Wang, C.H.; Zhu, G.S. Three pharmaceuticals cocrystals of adefovir: Syntheses, structures and dissolution study. *J. Mol. Struct.* **2015**, *1100*, 395–400. [CrossRef]
19. Llinas, A.; Barbas, R.; Font-Bardia, M.; Quayle, M.J.; Velaga, S.; Prohens, R. Two New Polymorphic Cocrystals of Zafirlukast: Preparation, Crystal Structure, and Stability Relations. *Cryst. Growth Des.* **2015**, *15*, 4162–4169. [CrossRef]
20. Hua, D.Y.; Chen, G.L.; Shen, W.J. Determination of two crystal forms of famotidine by differential scanning calorimetry. *J. Chin. Med. Ind.* **1991**, *22*, 78–79.
21. Wang, J.; Zhang, R.H.; Sun, S.Y. Study on the polycrystalline form of nimodipine. *Acta pharm. Sin.* **1995**, *30*, 443–448.
22. Jiao, L.T.; Zhang, L.; Yang, D.Z.; Yang, S.Y.; Du, G.H.; Lv, Y. Raman spectroscopic analysis and dissolution tests of nimodipine crystal forms. *Her. Med.* **2017**, *36*, 1175–1179.
23. Bao, J.Y.; Huang, H.; Yu, D.J.; Wei, W.; Jiang, Y.W.; Zhang, X.Q. Polymorphs of Istradefylline. CN104744464A, 1 July 2015.
24. Dong, D.D. The invention relates to a method for preparing Istradefylline crystal form III by ball milling. CN108117554A, 5 June 2018.
25. Wang, C.H. A new crystal form of Istradefylline and its preparation method. CN105884776A, 24 August 2016.
26. Gong, D.H.; Wang, J.; Gai, J.H.; Yang, J.; Sun, W.J.; Yang, M.; Yang, C.Q.; Ma, Y.X. A new crystal form of Istradefylline and its preparation method. CN106279169A, 4 January 2017.
27. Dong, D.D. A preparation method of Istradefylline crystal form II for treating Parkinson's disease. CN108101907A, 1 June 2018.
28. Bourne, S.A.; Villiers, M.D.; Crider, A.M.; Caira, M.R. Polymorphism of the antitubercular Isoxyl. *Cryst Growth Des.* **2011**, *11*, 4950–4957.
29. Cui, K.J.; Yang, Y.M.; Meng, Z.H.; Xu, G.R.; Xu, Z.B. Solubility of tetranitrodimerglycoluril (TNDGU) in different solvents at temperatures between 293.15 K and 313.15 K. *J. Chem. Eng. Data* **2014**, *59*, 2620–2622. [CrossRef]